ISSN: 2634-9221
European Journal of Applied Sciences; Vol. 14 No. 02 (2026) (01-13)
https://doi.org/10.14738/aivp.1402.20094

A Review of Polarized Light Microscopy in Food Science

Howard J. Swatland

1. Department of Animal Biosciences, University of Guelph

Abstract: Some of the basic principles of polarized light microscopy are explained, followed by the problems involved in making automated measurements for meat samples with automated pH changes. Polarized light microscopy is then applied to meat samples on a tilting microscope stage to separate diffuse subsurface reflectance from the gloss of surface reflectance, to explain what is happening when a slice of meat is examined at the macro level in a conventional colourimeter. When meat is cooked, tough connective tissues may be gelatinized, thus increasing meat tenderness. This may be detected by a loss of birefringence using a polarizing microscope. The optical basis of starch granules in polarized light is explained as an interaction of the radial crystalline structure of starch interacting with the rectilinear orientation of a microscope polarizer and analyser.

Keywords: Microscopy, Polarized light, Collagen, Gelatinization, Starch

INTRODUCTION

Polarimetry of solutions has a long history in food science, particularly for enantiomers of sugars, where it is a standard laboratory method [1]. But when it comes to ellipsometry of thin sections as seen under a microscope, we move from proven laboratory methods to speculative research. There are many food science research papers showing the Maltese Crosses of starch granules in polarized light. The authors of many of these papers write as if the Maltese cross might actually be embedded in the starch granule. For a start, the dark crosses on starch granules seen in polarized light have very little resemblance to heraldic Maltese Crosses with four “V” shaped arrows converging on a centre point. But the name is so well entrenched in food science literature it should remain undisturbed.

BASICS

The history of polarized light microscopy goes back much earlier than textbooks on microscopy will admit, right back to invention of photography. For anyone interested, search for Henry Fox Talbot (1800-1877) and David Brewster (1781-1868). Polarization allows a light microscope to detect structures smaller than the wavelength of light [2], not such a big thing in the modern world of atomic force microscopy but a bargain for any researcher working with limited funding. The main application of polarized light microscopy in food science is to study birefringent structures, those with two different refractive indices where, a transmitted light ray splits into two parts travelling at different velocities, the ordinary (o) and extraordinary (e) rays, with o $\perp$ e. Birefringence is measured as the refractive index (n) of the extraordinary ray minus that of the ordinary ray, and may be positive or negative in sign. An azimuth is an angle measured relative to a north-south axis of the microscope where the primary north-south axis divides the visible field into left and right sides and corresponds to a position of 0° on the first polarizer below the substage

condenser. Accessories added to a microscope may changes the orientation of the visible field, so that the 0° axis may be defined relative to the stand of the microscope [3]. From the 0° position, the convention of polar coordinates is to move counter clockwise to increment the angles. Points of the compass may also be used to describe the orientations of components, and are abbreviated to N, S, E and W. Relative to food structures examined with a polarizing microscope, the α or fast axis corresponds to the direction of the minimum refractive index, the minimum dielectric constant, and the maximum velocity. The γ or slow axis corresponds to the maximum refractive index, the maximum dielectric constant, and the minimum velocity. In special cases, a ß axis is recognized with intermediate properties between α and γ. When working with birefringent fibres such as collagen in meat, birefringence is usually taken as positive when the γ axis is parallel to the longitudinal axis of the fibre.

Sources of Birefringence

Birefringence may originate from molecular structure (intrinsic birefringence), such as an assemblage of parallel rod-like protein molecules. This is independent of the refractive index in which the sample is mounted. Another source of birefringence may be microstructural, such as an array of parallel fibres, and this does depend on the refractive index of the mounting medium [4]. Strain birefringence may originate from external forces acting on molecular structure [5]. In dynamic systems, flow birefringence may caused by shearing alignments of structures in a flowing system.

Retardation

Retardation is a decrease in the velocity of light caused by an interaction with the medium through which the light is passing. Phase retardation is an interference caused by ordinary and extraordinary rays diverging and taking different paths through the specimen (one path longer than the other). When the rays recombine after passing through the specimen they are out of phase by an amount equal to the path difference (between long and short paths). Thus, the path difference depends on both the degree of birefringence (divergence of paths) and the thickness of the specimen.

$$\text{phase retardation} = (n_e - n_o) \times \text{thickness}$$

Interference Colours

Interference colours caused by birefringence are shown by the Michel-Lévy colour charts found in mineralogy textbooks (Fig. 1), rather like the colours seen on a thin slick of oil on a puddle of water.

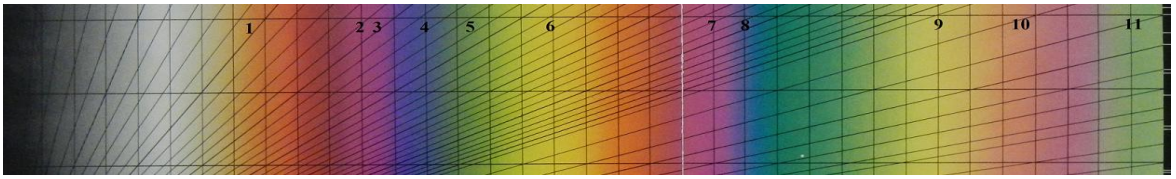

Fig 1: Interference colours from part of a Zeiss Michel-Lévy colour chart. The numbers show positions at which transmittance spectra were measured [6].

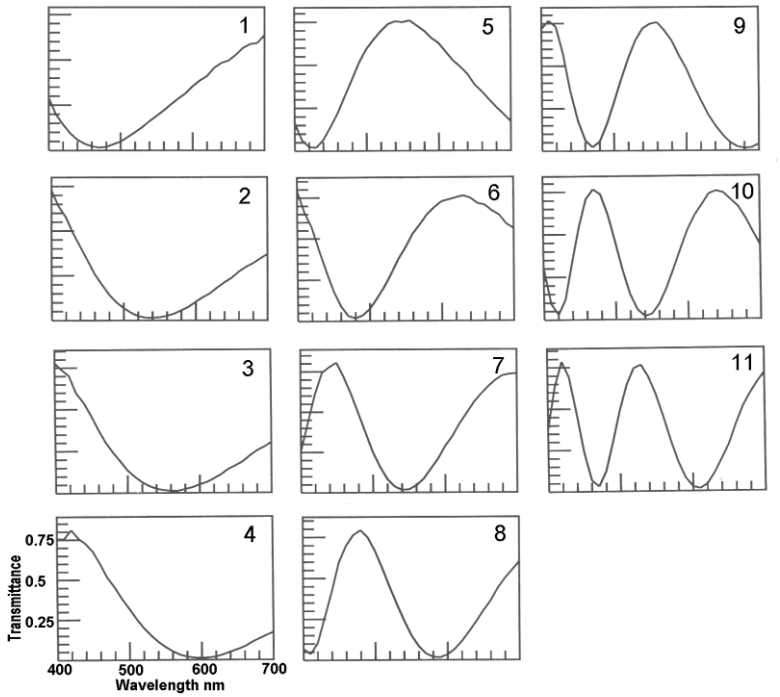

Fig 2: Transmittance spectra corresponding to positions in Fig. 1 [6].

The thinnest layer farthest from the source of the light on the oil is white, increasing to a red-orange (from zero to first order interference). Second order interference occurs with progressively greater thickness of the oil slick and ranges from purple through blue, green and yellow to orange-red. Third order interference follows a similar pattern, but the colours are misty and obscured, as when white light is added in pastel colours (Fig. 2). The colours range from violet, through sea-green and fleshy red, to dull purple. For the thickness at which biological tissues normally are dissected or sectioned with a microtome (≈ 10 μm), the birefringence of protein fibres like collagen is typically a first order white or pale yellow. The birefringence of foods systems is weak because of their high water when compared with the birefringence of minerals. The higher order colours of minerals may however be seen in very thick samples of foods.

Compensators

A polarizing microscope for transmitted light usually has a polarizer at a fixed azimuth beneath the substage condenser, and an analyzer in the microscope tube above the objective. A compensator may be inserted at 45° beneath the analyzer. Compensators such as the de Sénarmont are fixed in azimuth, and measurements are made with a rotary analyzer with a variable azimuth. For other compensators, the analyzer is fixed and the compensator is rotated or tilted to make measurements in the axis of the microscope. Especially when measuring small path differences in foods, objective measurements by photometry are preferable to subjective methods [7].

A small range compensator may be used after using a large-range compensator to find the maximum path difference. A calcite tilting Ehringhaus compensator may give the

maximum range (36.5 orders), below which a mica λ/4 de Sénarmont compensator may be used for first order interference as in most foods. It is very sensitive to the molecular causes of birefringence in biological structures [8]. A de Sénarmont compensator is a fixed quarter-wave plate oriented diagonally in a slider that inserts into a NW-SE slot below the analyzer, so that the final orientation of its γ axis is N-S.

CONTINUOUS MEASUREMENT OF BIREFRINGENCE

Problems arise when a sample has slowly changing birefringence in a food system because the operator may be influenced by the anticipated change [9]. Individual striated skeletal muscle fibres from beef samples were secured across a small metal frame (a paper clip) immersed in Sørensen's phosphate buffer. The sample was maintained in a small perfusion chamber with a depth of 3.5 mm.

If the muscle fibre moved away from the optical axis of the microscope, this changed the depth of the sample in the field and invalidated the path difference (because path difference depends on both birefringence and sample thickness). Similarly, if the orientation of the fibre changed, then the requirements for de Sénarmont ellipsometry were not satisfied. Thus, interrupt switches located near the microscope were incorporated to allow the operator to pause the program, adjust the specimen, and return to an earlier point in the measuring loop (before measurements were invalid). Another option was to terminate the measuring loop prematurely (if a fibre became loose or obscured by an air bubble). Thus, measurements were started under operator control and full automation was only used for stable samples. For a completely manual experiment with 20 measurements at each of 14 *p*H levels, the time required was essentially a whole working day (including data recording, calculations and graphical presentation of results). Using computer assistance, this was reduced to about 30 minutes once the sample was in position. The greatest advantage of computer assistance was objective determination of the extinction position [7].

Another problem was that if the muscle fibre underwent cytoskeletal disruption, allowing some fibrils to get out of register or kinked, instead of describing a sine wave, the signal became asymmetrical. At a low pH, the asymmetry was more conspicuous than at a high *p*H. In muscle fibres with orderly sarcomeres in their original arrangement, the signal obtained by rotating the analyzer was a symmetrical sine wave. The angle of the extinction position increased as the *p*H decreased so that, as confirmed independently using a polarised-laser ellipsometer, muscle birefringence increases as *p*H is decreased [10]. But problems also arose from the effect of *p*H on muscle fibre diameter. There was approximately a 15% decrease in diameter as *p*H decreased from about *p*H 7 to 5.5. Because of this bias, the changes in path difference may be underestimates of the path difference for a constant thickness of muscle.

This apparently trivial experiment using a shred of meat attached to a paper clip [9], was the first explanation for something meat scientists had long agreed on, ever since *p*H meters had first been applied to meat in the 1930s and 1940s. Everyone agreed that meat with a low *p*H was pale relative to meat with a high *p*H which was dark. There were numerous distractions related to myoglobin content and the genetic and behavioural basis for why some animals produced lactate more rapidly than others. But how did *p*H cause changes in light scattering, pale versus dark? By a fortunate coincidence, myofibrils are

birefringent and may be examined by polarized light microscopy. As seen in Fig. 3, birefringence peaks at a low *p*H to create a high degree of light scattering and pale meat, while birefringence is low at a high *p*H in dark meat. This may not be the ultimate answer to why meat with a low *p*H tends to be more pale than meat with a high *p*H. Let us wait for a better explanation, but this does explain how light scattering affects meat colourimetry and is correlated with fluid losses from meat [11]. At least, it does show how polarized light microscopy can reveal something of interest in meat science.

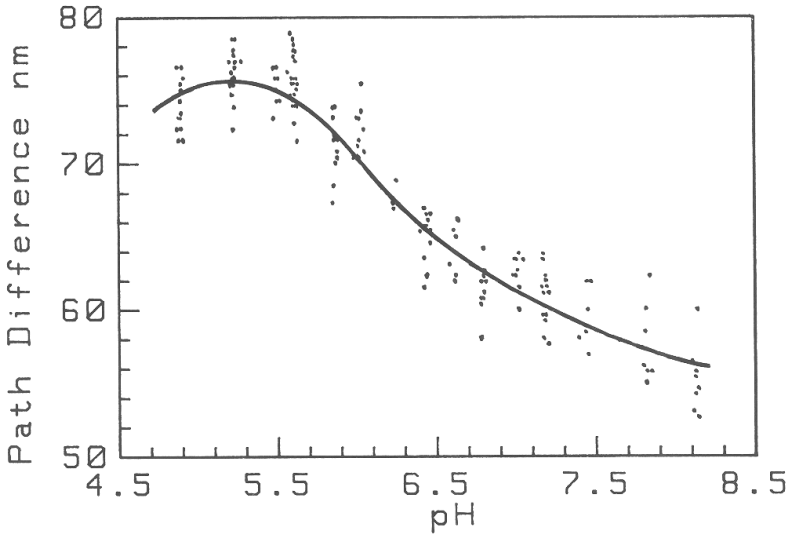

Fig 3: The birefringent path difference of a beef muscle fibre using an automated microscope and an automated *p*H changer [9].

REFLECTED LIGHT

While polarized light microscopy has many applications in materials science, it could be used more widely in food science, as in bread making [12]. Many solid foods are both translucent and glossy, and separating the two is important. Reflected light may contain diffuse, sub-surface scattering, plus glossy surface reflectance following Fresnel equations for polarization of reflections at a boundary [13]. If a commodity is heterogeneous in composition, each component may have its own optical properties, but these are averaged by conventional techniques of colourimetry, which typically integrate an area of several square centimetres. This is an ideal problem for investigation with the polarizing microscope using a tilting stage.

There are special problems in the examination of food samples with a tilting stage [14]. From Brewster's law, the polarization angle (Θ) of reflected rays is related to refractive index (n), $n = \tan \Theta$, but the refractive index of tissue fluids may be quite variable. Furthermore, whereas overall surface reflectance may indicate sample boundary conditions, such as surface wetness or smoothness, its spatial pattern may indicate intrinsic structure, such as plant cells walls, globular fat droplets, or biological fibres. A final complexity is that tissues such as muscle, may sometimes exhibit natural iridescence from destructive interference.

In Fig. 4, the area of the specimen illuminated by the optical fibre is shown as an ellipse, with a long axis, AB. The axis of rotation of the tilting stage corresponded to the

short axis of the illuminated ellipse. Thus, the optical axis of the optical fibre (OF), and the long axis (AB) of the illuminated ellipse defined the plane of incidence.

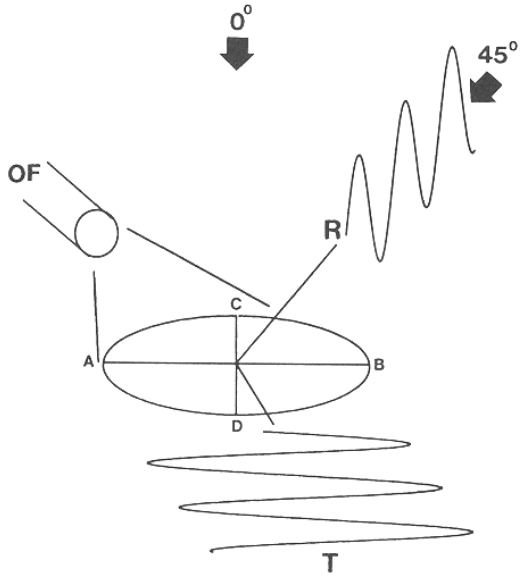

Fig 4: Examining a food sample on a tilting stage of a polarizing microscope using lateral illumination from an optical fibre moving with stage (OF) and measuring reflectance (R) and transmittance (T) [14].

The efficiency of polarizers and analyzers in a microscope may be checked by measuring their extinction coefficients at different wavelengths,

$$k = \log_{10} (T_0 / T_{90})$$

where T_0 is with the analyzer parallel to polarizer, and T_{90} is with the analyzer perpendicular to the polarizer. A similar approach may be used to find the degree to which light reflected from samples is polarized, using reflected light rather than transmitted light, and replacing the polarizer by the sample. Thus,

$$k = \log_{10} (R_0 / R_{90})$$

so that a high extinction coefficient indicates a strong polarizer, and vice versa. A subscript is used to denote the angle of tilt at which k was measured.

When using a polarizing microscope, there is always a risk that some unseen factor has created internal optical anisotropy which, if accepted uncritically, might wrongly be attributed to the sample. If a diffuse white sample, such as opal glass, is illuminated from above with non-polarized light through an epicondenser, one would not expect rotation of the analyzer to cause much change in reflectance detected by the photometer. If this did occur, the source of the unwanted polarization could be either before the analyzer (so that light reaching the analyzer was partly polarized), or after the analyzer (so that the analyzer was polarizing the light, which then was interacting with an optically anisotropic component in, or beneath the photometer). Opal glass with very low gloss and Teflon (polytetrafluoroethylene) with appreciable gloss may be used as white samples to check for intrinsic optical anisotropy in the microscope [15].

In a translucent food system containing a myriad of scattering particles, the light path through which absorbance occurs is greatly increased by scattering [16]. Thus, the degree of absorbance becomes an interaction between the concentration of the chromophore and the lengthening of the light path by scattering. In addition, for tissues such as skeletal muscle, surface reflectance may be anisotropic, with a higher reflectance when the incident illumination is perpendicular to the muscle fibres than when it is coaxial. Unfortunately, the pioneer work in reflectance spectroscopy of intact tissues by Ray and Paff [17] did not receive the attention it deserved, and it was not until the advent of fibre-optic spectroscopy that work was resumed in this area.

Myoglobin is the dominant chromophore of skeletal muscle and determines the reflectance spectrum of meat. When myoglobin and its derivatives have been removed by washing, reflectance is almost a linear function of wavelength (from about 0.3 at 420 nm to about 0.75 at 700 nm). The Soret absorbance bands for deoxymyoglobin (purple-red), oxymyoglobin (bright-red), and oxidised metmyoglobin (brown) are at 434, 416 and 410 nm, respectively [18]. Deoxymyoglobin has an absorbance band at 555 nm that is replaced in oxymyoglobin by a strong absorbance band at 578 nm and a slightly weaker band at 542 nm, although metmyoglobin formation generally masks this difference between reflectance at 542 and 578 nm. The relatively high myoglobin concentration of the dark red skeletal muscle reduces the overall intensity of reflectance spectra to about one third that of washed muscle or a white muscle lacking myoglobin.

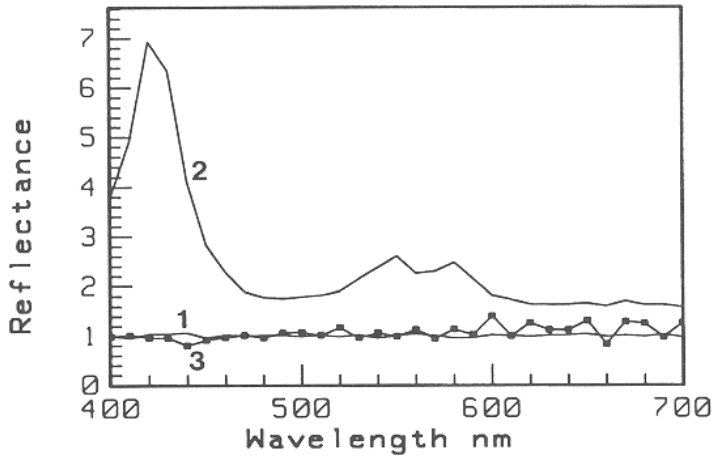

Fig 5: Tilting red muscle in a polarizing microscope with a tilt of 45° (line 1), 90 ° (line 2), and then the analyzer rotated to 90° (line 3) [19].

With a polarizing microscope standardized on a sample of dark red muscle (to give reflectance ≈ 1 from 400 to 700 nm) at 0° tilt and 0° analyzer (Fig. 5, line 1), when the stage was tilted to 45°, reflectance increased at 420 nm and at 550 and 580 nm (Fig. 5, line 2). When the analyzer was rotated to 90° (thus removing most of the surface reflectance added when the stage was tilted), reflectance returned almost to initial values (Fig. 5, line 3). Line 2 of Fig.4 has almost the same shape as an absorbance spectrum of oxymyoglobin. In diffuse light, some wavelengths are less intense than others because scattering is a function of wavelength, or because of selective absorbance of certain wavelengths. When surface reflectance is added to diffuse light by tilting a sample, its spectral composition is

determined by the emission spectrum of the illuminator, thus adding light at wavelengths that may be weak in the diffuse light used for standardization. Hence, line 2 in Fig. 4 follows the absorbance spectrum of oxymyoglobin, the dominant myoglobin derivative in the muscle. Removing much of the surface reflectance by rotating the analyzer caused reflectance to return near to the values at standardization (Fig.4, line 1).

The fibres of both muscle and tendon are bound into a fascicular structure, creating a directional grain on the sample surface. When an area for measurement was relatively flat, the results of tilting the sample were predictable. But when bundles of either muscle fibres or collagen fibres rolled through the optical axis they gave a flash of surface reflectance into the optical axis, and a corresponding flash of strongly polarized surface reflectance. The effect was strongest when the fibres were parallel with the axis of rotation of the tilting stage. Apart from this effect, polarization was generally low in areas of the muscle and tendon with a low surface reflectance, and high in areas with high surface reflectance ($k_{45} \approx 0.14$ and $k_{45} \approx 0.68$, for dull and glossy areas, respectively). Muscle and tendon specimens with both an appreciable gloss and a fascicular grain acted as partial polarizers, even at 0° tilt ($k_0 \approx 0.05$). In other words, the sides of fibres protruding from the sample surface already were tilted relative to the optical axis of the microscope, so that reflected light was partly polarized.

CONNECTIVE TISSUE

Collagenous connective tissues are the main reason that different cuts of beef and lamb differ in price, with a premium given to the cuts with a low content of connective tissue producing tender meat. The strongest and most heat resistant fibres are those of biochemical type I with a tropocollagen structure of $[\alpha1(1)]_2\alpha2(I)$. Their intrinsic and form birefringences are both strong and positive in sign [20].Collagen fibres in meat occur around individual muscle fibres (endomysium), around bundles of muscle fibres (perimysium) and around whole muscles (epimysium). From meat samples frozen in liquid nitrogen, thin (10 µm) sections may be cut with a cryostat and heated on a microscope hot stage to find the temperature at which gelatinization occurs and birefringence is lost.

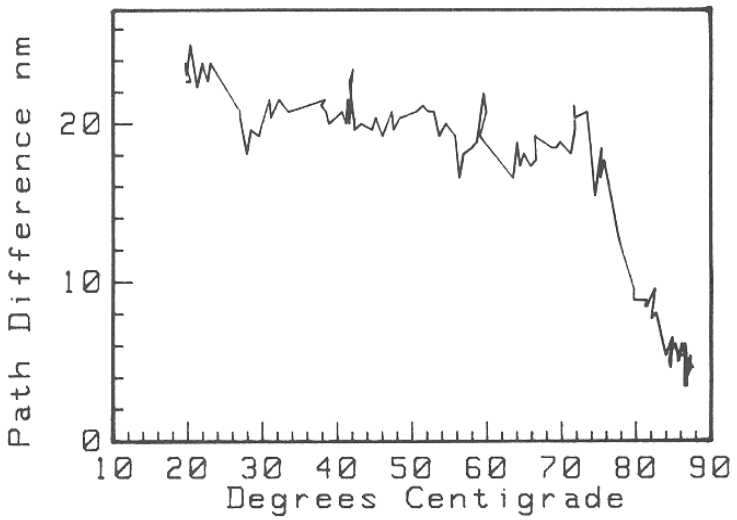

Fig 6: Automated measurement of path difference of perimysium in pork *longissimus dorsi* on an automated microscope hot stage [21].

In Fig. 6, gelatinization is just above 76° where there is a sharp drop in birefringence. A critical viewing of Fig. 6 may question the irregularities from 20° to 70° which are result of automation. Thus, there are a couple of places with small reversals in temperature – perhaps air movement over the microscope slide? Variation in path difference might be caused by the electromechanical errors of rotating an analyzer to find the extinction position with a de Sénarmont compensator – who knows? But it might also be that the system is detecting birefringence changes prior to gelatinization. Gelatinization of connective tissue in meat is quite complex, with both time-temperature interactions compounded by contraction and changes in light scattering [22].

STARCH

Getting back to the starting point of this review, the isogyres (dark shadows in interference figures) of a Maltese cross in a starch granule are dependent on the orientation of the polarizer and analyzer in a microscope. If both polarizer and analyzer are rotated in tandem, the Maltese cross rotates as well. Figure 7 shows isogyres on a starch granule in white light (top left 0°), but the rest of the figure shows the same starch granules with a phase shift from a Nikitin-Berek tilting compensator. Interference colours may reveal something about the structure of starch granules [24-26] but what determines the quadrants seen in Fig. 7?

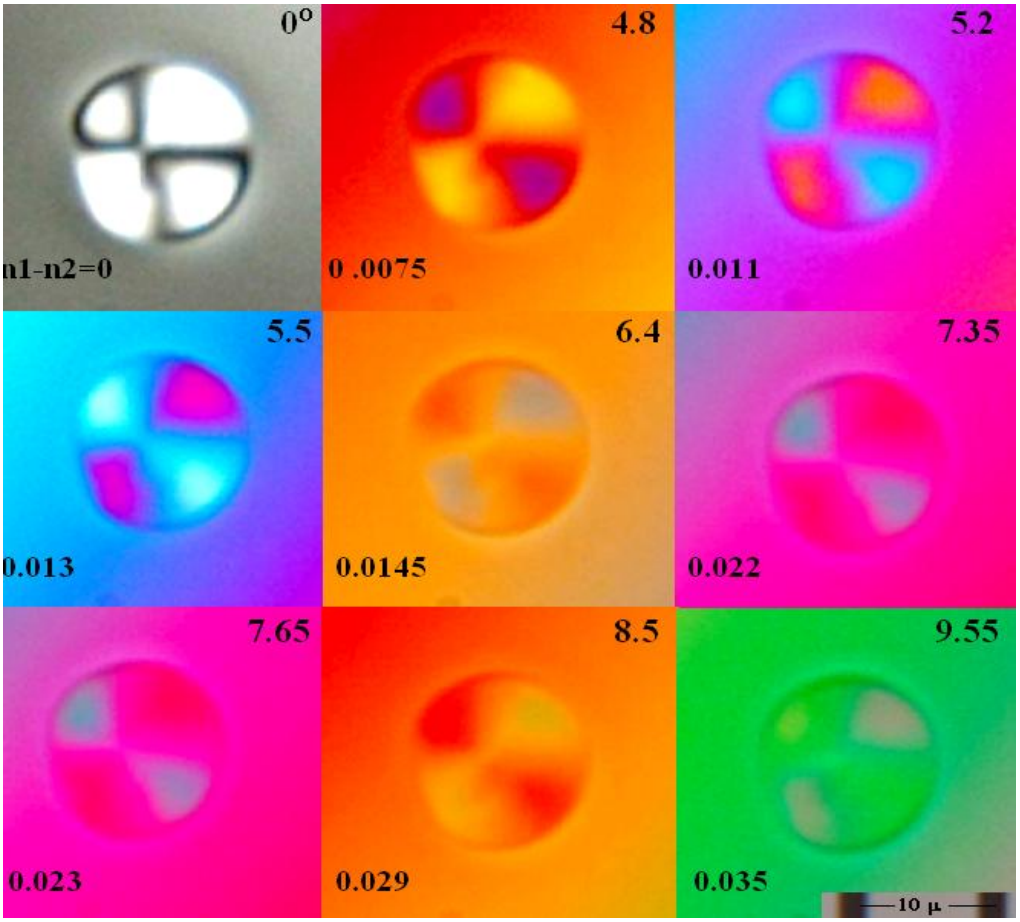

Fig 7: The isogyres (Maltese cross) of a high-amylose corn starch granule viewed in white light without a compensator tilt (top left, n1- n2 = 0 at 0° tilt), and then the interference colours as the compensator was tilted [23].

Just as the history of polarized light microscopy goes back earlier than microscopy text books will admit, so does the microscopy of starch granules. There was a time when starch granules were used to adulterate natural drug powders, but this was detectable by polarized light microscopy. Jonathan Pereira in 1843 [27] reported that if starch granules were viewed against a background interference colour they had a quadrant of diagonally paired interference colours, one pair adding, and one pair subtracting from the background interference. Starch granule size is important industrially [28] but it is fundamental in the polarized light microscopy of starch granules. Everything in the polarized light microscopy of minerals depends upon the thickness of the sections examined. Figure 1 shows a small part of a Michel-Lévy colour chart, the rest of the chart shows the same interference colours with a grid determined by section thickness allowing different minerals to be identified by their birefringence. So how can we use this method with starch granules? The obvious answer is the diameters of the starch granules must be measured to estimate the path difference through the granule.

The quadrant of inference colours discovered by Jonathan Pereira in 1843 [27] are explained by the radial structure of starch [30]. Thus, some radii are in line with the axis of the compensator while others are across the compensator axis. Where radial birefringence counteracts the background birefringence, starch granules may have two quadrants with a bright yellow first-order interference colour. Where radial birefringence is added to the background birefringence, there may two quadrants of second-order blue (higher than the background). In yellow quadrants where birefringence is reduced, the wavelength of the first interference minimum is reduced. In blue quadrants where birefringence is increased, the wavelength of the first interference minimum is increased. The extent to which the interference minimum of the background birefringence is shifted by starch granules is strongly dependent on the size of the starch granules. For yellow quadrants the shifts are: r = -0.87, P < 0.001, n = 22, for corn starch; r = -0.94, P < 0.001, n = 22, for tapioca starch; and r = -0.94, P < 0.001, n = 12, for potato starch. For blue quadrants the shifts are: r = 0.80, P < 0.001, n = 22, for corn; r = 0.81, P < 0.001, n = 22, for tapioca; and r = 0.93, P < 0.001, n = 16, for potato [29]. Thus, when interference colours are used to evaluate starch granules, the granules should be similar in size or a correction must be made for granule size.

Figure 7 supports Pereira's discovery [27], but colour perception is in the mind of the observer and some quantitative data might help prove the point. With hindsight, knowing now the radial molecular structure of starch granules [30], this seems reasonable. It might have been discovered a century ago, just as the sliding filament theory of muscle contraction might have been discovered a century ago from polarized light microscopy [31]. But there should be no complacency, we still do not understand in the geosciences how the radial structure of vaterite (an unstable crystal of calcium carbonate) is converted to rectilinear calcite or aragonite [32].

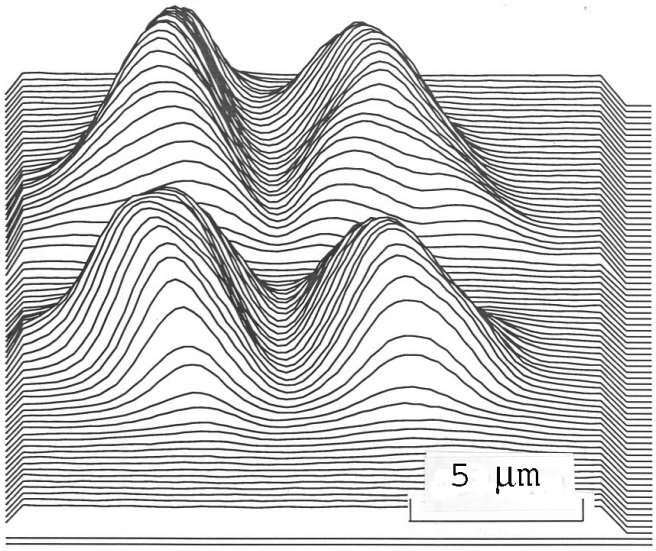

Fig 8: Transmission peaks for a quadrant from a corn starch granule in white light [20].

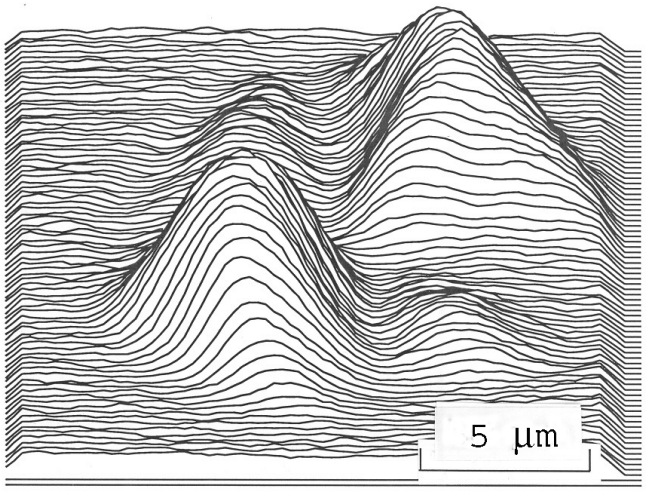

Fig 9: Transmission peaks for Fig. 8 in monochromatic light (550 nm), diagonal yellow quadrants are suppressed [20]

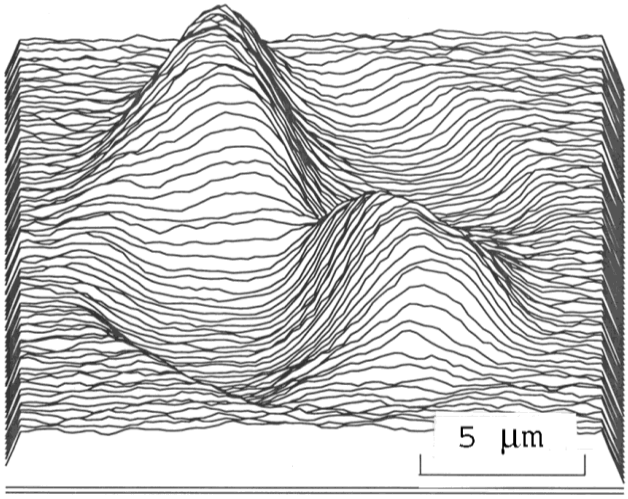

Fig 10: Transmission peaks for Fig. 8 in monochromatic light at 650 nm, diagonal blue quadrants are suppressed [20].

REFERENCES

[1] Cescon, I. and Stefanel A. (2022). Polarimetry measurement in a physics lab for food science undergraduate students. Physics Teacher. 60: 144-148.

[2] Arimoto, R. and J. M. Murray. (1966). Orientation-dependent visibility of long thin objects in polarization-based microscopy. Biophysics Journal. 70: 2969-2980.

[3] Bennett, H. S. (1950). Methods applicable to the study of both fresh and fixed material. The microscopical investigation of biological materials with polarized light. In: R. McClung Jones (ed.) McClung's Handbook of Microscopical Technique. Paul Hoeber, New York. 3rd edit. pp. 591-677.

[4] Pimentel E.R. (1981). Form birefringence of collagen bundles. Acta Histochemica et Cytochemica . 14: 35-40.

[5] Chien, J. C. W. and Chang, E.P. (1972). Dynamic mechanical and rheo-optical studies of collagen and elastin. Biopolymers. 11: 2015-2031.

[6] Swatland, H.J. (2015). Interference colourimetry of starch granules. Color Research and Application. 41: 352-357.

[7] Roche, E. and Van Kavelaar , R.F. (1989). Photometric measurement of small optical path differences. Journal of Microscopy. 157: 181-186.

[8]. Nollie, G.J., Sandhu, H.S., Cernovsky, Z.Z. and Canham, P.B. (1996). Regional differences in molecular cross-linking of periodontal ligament collagen of rat incisor, by polarizing microscopy. Connective Tissue Research. 33: 283-289.

[9]. Swatland, H.J. (1990). Effect of pH on the birefringence of skeletal muscle fibers measured with a polarizing microscope. Transactions of the American Microscopy Society. 109: 361-367.

[10] Yeh, Y., Baskin, K., Burton, K. and Chen, J.S. (1987). Optical ellipsometry on the diffraction order of skinned fibers: pH-induced rigor effects. Biophysics Journal. 51: 439- 447.

[11] Swatland, H.J. Optical properties of meat. (2012). Proceedings of the Reciprocal Meat Conference, Fargo, North Dakota.

[12] Marchant, J.L. and Blanshard, J.M.V. (1978). Studies on the dynamics of gelatinization of starch granules employing a small angle light scattering system. Stärke. 30: 257-264.

[13] Judd, D.B. and Wyszecki, G. (1975). Color in Business Science, Science and Industry. John Wiley, New York.

[14] Swatland, H.J. (1995). Surface reflectance of meat measured by microscope polarimetry using a tilting stage with lateral illumination. Journal of Computer Assisted Microscopy. 7: 211-219.

[15] Weidner, V.R. and Hsia, J.J. (1981) Reflection properties of pressed polytetrafluoroethylene powder. Journal of the Optical Society of America. 71: 856-861.

[16] Butler, W.L. (1962). Absorption of light by turbid materials. Journal of the Optical Society of America. 52: 292-299.

[17] Ray, G.B. and Paff, G.H. (1930). A spectrophotometric study of muscle hemoglobin. American Journal of Physiology. 94: 521-528.

[18] Bowen, W.J. (1949). The absorption spectra and extinction coefficients of myoglobin. Journal of Biological Chemistry. 179: 235-235.

[19] Swatland, H.J. (1995). Surface reflectance of meat measured by microscope polarimetry and spectrophotometry using a tilting stage. Journal of Computer-Assisted Microscopy. 7: 211-219.

[20] Romhányi, G. (1986). Specific topo-optical reactions of connective tissue elements and their ultrastructural interpretation. Connective Tissue Research. 15: 13-16.

[21] Swatland, H.J. (1990). Thermal denaturation of perimysial collagen in meat measured by polarized light microscopy. Journal of Food Science. 55: 305-307.

[22] Swatland, H.J. (2006). Thermal denaturation of bovine longissimus thoracis aponeurosis, correlating contraction with optical changes. Canadian Journal of Animal Science. 86: 221-224.

[23] Swatland, H.J. (2016). Starch granules in polarized light, following Pereira into the ultraviolet. Quekett Journal of Microscopy. 42: 601-609.

[24] Seckinger, H.L. and Wolf, M.J. (1966). Polarization colors of maize starches varying in amylose content and genetic back-ground. Stärke*, 18,* 2-5.

[25] Evans, A., McNish, N. and Thompson, D.B. (2003). Polarization colors of lightly iodine-stained maize starches for amylase-extender and related genotypes in the W64A inbred line. Stärke, 55, 250-257.

[26] Evans, A. and Thompson, D. B. (2004). Resistance to α-amylase digestion in four native high-amylose maize starches. Cereal Chemistry, 81, 31-37.

[27] Pereira, J. (1854). The Elements of Materia Medica and Therapeutics. Longman, London.

[28] Lindeboom, N., Chang, P.R. and Tyler, R.T. (2004). Analytical, biochemical and physicochemical aspects of starch granule size, with emphasis on small starch granules: a review. Stärke 56, 89-99.

[29] Swatland, H.J. (2009). Effect of granule size on the interference colors of starch in polarized light. Biotechnic and Histochemistry. 84: 329-336.

[30] Frey-Wyssling, A. (1969). On the molecular structure of starch granules. American Journal of Botany. 56, 696-701.

[31] Galler, S. (2015). Forgotten research from 19th century science should not follow fashion. Journal of Muscle Research and Cell Motility. 36: 5-9.

[32] Swatland, H. J. (2010). Polarized-light interferometry of calcium carbonate deposition in moss from a waterfall on the Niagara Escarpment. Microscopy and Microanalysis. 16: 306-12.